CANMET

REPORT 78–10

Canada Centre for Mineral and Energy Technology

Centre canadien de la technologie des minéraux et de l'énergie

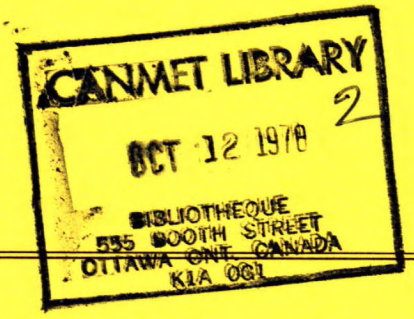

BLOCK FLOW SLOPE INSTABILITY

D.F. COATES AND Y.S. YU

MINERALS RESEARCH PROGRAM
MINING RESEARCH LABORATORIES

Energy, Mines and Resources Canada
Énergie, Mines et Ressources Canada

JUNE 1978

Available by mail from:

Printing and Publishing
Supply and Services Canada,
Ottawa, Canada K1A 0S9

CANMET
Energy, Mines and Resources Canada,
555 Booth St.,
Ottawa, Canada K1A 0G1

or through your bookseller.

Catalogue No. M38-13/78-10
ISBN 0-660-10019-3

Price: Canada: $1.00
Other countries: $1.20

Price subject to change without notice.

En vente par la poste:

Imprimerie et Édition
Approvisionnements et Services Canada,
Ottawa, Canada K1A 0S9

CANMET
Énergie, Mines et Ressources Canada,
555, rue Booth
Ottawa, Canada K1A 0G1

ou chez votre libraire.

Nº de catalogue M38-13/78-10
ISBN 0-660-10019-3

Prix: Canada: $1.00
Autres pays: $1.20

Prix sujet à changement sans avis préalable.

BLOCK FLOW SLOPE INSTABILITY

by

D.F. Coates* and Y.S. Yu**

ABSTRACT

When structural conditions of a slope do not favour plane shear sliding, or the rock mass is not sufficiently ductile to permit rotational sliding, slope instability, if it occurs, must be due to breakdown of the rock substance. The breakdown would be initiated at points of high stress. After local crushing, the load is transferred to adjacent zones, subjecting them to excessive stress and leading to further crushing. Consequently, crushing of rocks at points of high stress is the pertinent failure mechanism.

Rational analysis for this type of slope instability — local crushing or progressive failure — is not fully developed at present and obviously much research work has to be done before a useful engineering tool is established. In spite of this difficulty, however, an analysis procedure with examples is suggested based on a probabilistic approach making use of the best available information on stress conditions in a slope and material properties of the rock mass. This in turn will provide a means of appraising the effects of incremental slope changes on benefits and costs.

---

* Director-General, Canada Centre for Mineral and Energy Technology (CANMET), Energy, Mines and Resources, Canada, Ottawa, Canada

** Research Scientist, Mining Research Laboratories, CANMET, EMR, Ottawa, Canada

INSTABILITE DE LA PENTE PAR L'ECOULEMENT EN BLOC

par

D.F. Coates* et Y.S. Yu**

RESUME

Lorsque les conditions structurales d'une pente ne favorise pas le glissement par cisaillement plan ou que la masse rocheuse n'est pas suffisamment ductile pour permettre le glissement circulaire, l'instabilité de la pente, si cela se produit, doit donc être causée par une détérioration de la substance rocheuse. Cette détérioration débute aux points soumis à une haute tension. La charge est transmise aux zones adjacentes après l'écrasement local, les soumettant ainsi à une tension excessive occasionnant un écrasement additionnel. En conséquence, l'écrasement des roches aux points soumis à de hautes tensions consiste un mécanisme de défaillance important.

Pour l'instant, l'analyse rationnelle de ce genre d'instabilité de la pente — écrasement local ou défaillance progressive — n'est pas suffisamment perfectionnée et pour mettre au point un outil technique utile, il faudra certainement intensifier les recherches dans ce domaine. Malgré les difficultés rencontrées, un procédé d'analyse y compris quelques exemples, suggère l'utilisation de données de probabilité faisant appel à l'information disponible sur les conditions de tension d'une pente et des caractéristiques du matériau de la masse rocheuse. Ceci permettra d'évaluer les effets de variations dans les pentes sur les avantages et les coûts d'opération.

---

* Directeur-général, Centre canadien de la technologie des minéraux et de l'énergie (CANMET), Ministère de l'Energie, des Mines et des Ressouces, Ottawa, Canada

** Chercheur scientifique, Laboratories de recherches sur les mines, CANMET, EMR, Ottawa, Canada

CONTENTS

TABLES

FIGURES

INTRODUCTION

In some pit walls, instability if it occurs, must be due to breakdown of the rock substance. In this case, structural conditions do not favour plane shear sliding, and the rock substance is not sufficiently ductile to permit rotational sliding. Consequently, crushing of the rock at points of highest stress is the pertinent mechanism.

After such local crushing, the load is transferred to adjacent zones subjecting them to excessive stress and leading to further crushing. This progressive action, which can be observed in the working and deforming of some slopes before major movement takes place, continues until a general breakdown of the rock mass occurs with a flow of broken rock.

Zones of maximum stress in the slope can arise from various causes. In a homogeneous formation, stress trajectories could be expected to be substantially as shown by the models in Fig. 1 and 2. The deflection of the stress around the toe of the slope results in a concentration in this area similar to the notch effect in structural members. This stress concentration may result in crushing and lead to instability.

It can be seen from Fig. 1 and 2 that the notch effect is slight where the field stresses are due only to gravity, i.e., when horizontal stresses are a fraction of the vertical stresses. On the other hand, with larger horizontal stresses due to tectonic action the notch effect is more significant.

The models used to determine the stress distributions described above were elastic and

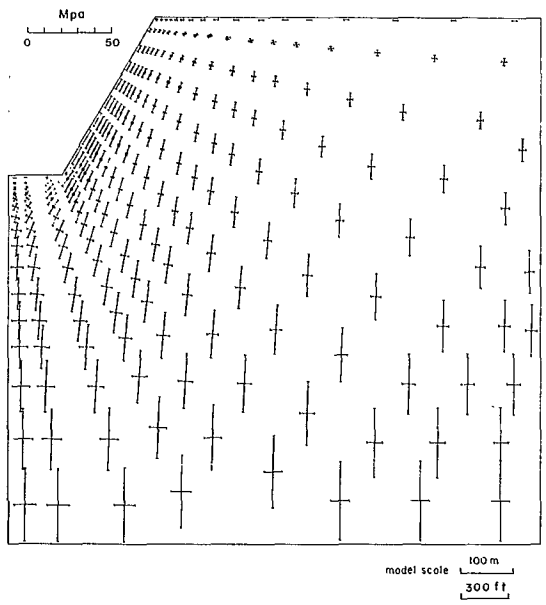

Fig. 1 - Principal stresses in a 60° slope finite element model where the horizontal field stresses are one-third of the vertical stresses; the long bars of the crosses represent the magnitude and direction of the maximum compressive stress; the short bars represent the minimum compressive stress; note how the maximum stresses flow parallel to the slope face and then around the toe

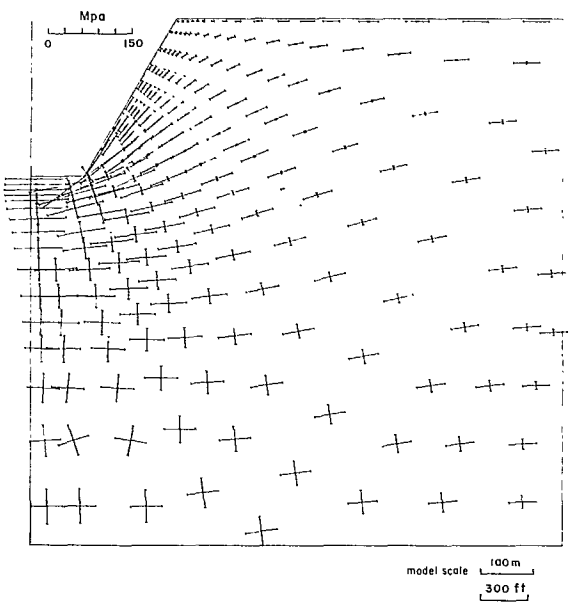

Fig. 2 - Principal stresses in a model of a 60° slope where the horizontal field stresses are three times greater than the vertical stresses; note crowding of the flow of stress around the toe, producing more stress per unit area or a concentration of stress

homogeneous. These assumptions are not usually valid for real slopes. However, the stress flow in real slopes must have some similarity to these idealized patterns. The differences are analogous to the differences in the flow of water in a rocky stream compared with that in a regular, smooth channel in a laboratory.

Stress concentrations in slopes also occur where rocks of differing stiffness exist in a slope. In one case, a thin strong layer of quartzite occurs in the footwall of a series of predominantly schistose rocks. The quartzite layer is much stiffer than the adjacent layers. Excavation of the open pit will cause stress concentrations something like that shown in Fig. 3. The quartzite will be subjected to stresses approximately five times greater than those in the adjacent schist layers. Because the strength of the quartzite is only about twice that of the schist, crushing would occur first in the quarzite. For a slope that is high enough instability could thus be initiated in the quartzite layer and could spread progressively to the adjacent rocks creating a slide in the wall.

Figures 4 and 5 show the cracking and upheaval that occurred in the bottom of a pit some 100 ft (30 m) out from the toe of a slope 300 ft (91 m) high. Part of the cause of this movement was probably due to concentration of the horizontal stress being deflected around the toe of the

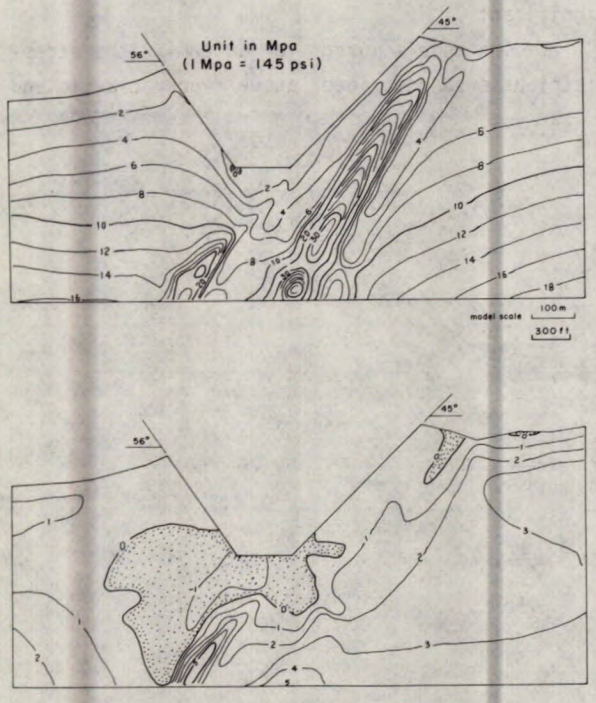

Fig. 3 - A finite element model of a prospective open pit; the footwall, on the right, consists mainly of schistose layers but also contains a layer of hard quartzite that is much stiffer than the others; as the pit is excavated the stiff quartzite can be expected to take more than its share of the load from the slope; the contours of equal maximum compressive stress shows the concentration of stress in the quartzite to be some five times greater than that in the adjacent layers

Fig. 4 - Cracking 100 ft (30 m) beyond the toe of a 300-ft (91-m) high wall

Fig. 5 - Some 4 ft (1.2 m) of heave beyond the toe of a 300-ft (91-m) wall

slope as shown in Fig. 2. Structural features undoubtedly also played a part in the resulting action. The case could not be analyzed because of lack of data.

A similar reaction is shown in Fig. 6 where upheaval of some 8 ft (2.4 m) occurred during stripping in horizontally bedded limestone. It is possible that the high horizontal stresses in the pit bottom caused the first layer to buckle in a manner similar to buckling of a long thin column. Without field stress measurements and detailed information on the geometry, jointing and bonding of the layers, it was not possible to analyze this hypothesis.

Figure 7 shows a slope 445 ft (136 m) high at an average angle of 51° which broke down producing a substantially uniform mass of rubble. No plane shear surfaces were evident. It is assumed that this was a case of block flow instability where the breakdown had been caused by crushing of the rock substance. It is known that the horizontal stresses in this formation were greater than the vertical stresses and that the strength of the rock substance varied widely depending on the degree of alteration and weathering. By making assumptions regarding the field stresses and effects of weathering on the dispersion of strength, it was calculated that the probability of this failure occurring was about 5%. This was substantially corroborated by experience when

Fig. 6 - An upheaval of 8 ft (2.4 m) and cracking of the floor in an open pit during stripping indicated the presence of high horizontal stresses in the formation

mining along many thousand feet of this wallrock through three pits, and obtaining this degree of instability.

Another reaction of wallrocks to excavation is deformation. The removal of ground releases stresses or pressures that were acting on the pit floor and wall faces before excavation. Removing these constraints results in a tendency for the floor to rise and for the walls to move inward as shown in Fig. 8. In model studies when the field stresses are due only to gravity, the crest of the slope moves upward and away from the pit. When horizontal field stresses due to tectonic action are greater than the gravitational induced stresses, the crest moves downward and towards the pit. However, these models are for elastic, homogeneous and continuous ground; structural discontinuities modify these movement patterns. The general effect of having a discontinuous mass is to add large components of downward and inward movement; local effects of particular structural features will also occur. From the point of view of stability, these deformations might be significant because they result in loosening of the rock mass. Insufficient research has been done at the present, hence movement of walls when mining out the ore would be worth measuring to provide a basis for predicting the onset of instability.

Fig. 7 - Slope instability caused by toe crushing; a slope 445 ft (136 m) high at 51° failed in a manner suggesting initiation was by toe shearing followed by a general breakdown of the rock mass

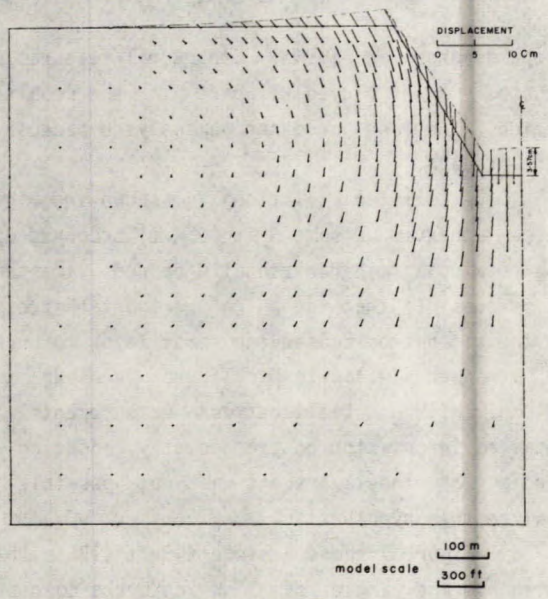

Fig. 8 - A finite element model showing the deformations resulting from excavation of an open pit; in this case, the field stresses are due only to gravity (i.e., K = 1/3); for a depth of 980 ft (300 m) the pit floor would heave, in effect, be lifted 35.7 mm, assuming the modulus of deformation of the rock is 10 x 10^6 psi (69 x 10^6 KPa)

DESIGN

In a homogeneous elastic slope, maximum compressive stress will occur at the toe of the slope owing to the notch effect as illustrated in Fig. 1 and 2. Away from the toe the stresses will decrease. Consequently, if any crushing occurs it will usually start at the toe. Figure 9 shows the magnitude of toe stresses obtained in a series of models for different slope angles and different ratios of horizontal to vertical field stresses. The stresses at the toe increase with the slope angle.

To determine toe stresses and other zones of concentration of stress, the finite element method is available. This numerical solution must be used because no theoretical solution exists for wall geometry. The results must be considered as rough estimates of actual stresses.

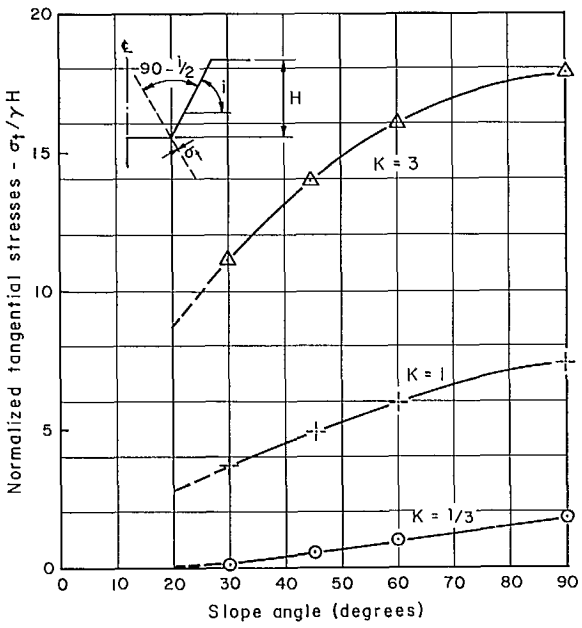

Fig. 9 - Variation of toe stresses, σ_t, with slope angle and K, the ratio of horizontal to vertical field stress, under plane strain conditions; γ is the density of the rock mass in the wall; H is the height of the slope; σ_t is at a point approximately 2 m in from the rock surface

To simulate pit walls, modeling to some extent can include the variation in deformation properties of the different formations and also the deformation properties of some of the discontinuities that have been identified in the field investigation. Homogeneous field stress conditions of tectonic origin can also be included. Where appropriate, the effects of ground water flow into the pit can be included in the analysis, although hydraulic pressure would not normally influence breakdown of the blocks of rock at the toe unless it were through an alteration mechanism.

Where it is impractical to run a series of finite element studies, the curves of Fig. 9 to 15 can be used to provide information on the relative effects of slope height and angle. These curves were constructed from models with certain dimensions, such as the distance from the face to the point inside the rock block where the stress is assumed to occur, the distance to the vertical model boundary from the slope face, and the width of the pit bottom (1). Different model dimensions would produce somewhat different stresses. Furthermore, the selection of the dimensionless ratios on the y-axis for including the effects of all the parameters is somewhat arbitrary. A different scaling law would produce somewhat different design results.

Using these curves requires some knowledge of the field stress regime in the rocks around the pit, which is not easily obtained at the present stage of development of rock mechanics. A best effort must be made to obtain such information, but in some circumstances this might consist of a geologist's study of the tectonic history and guessing at the present stress regime.

The strength of the rock substance in the blocks bounded by joints and other discontinuities is required for this design analysis. The mean and standard deviations of the uniaxial compressive strength must be determined. Tests on samples of varying sizes can be used to extrapolate to blocks of larger volume. In brief, the procedure is to establish the relation between mean compressive strength and volume of sample, and then to extrapolate this relationship to the volume of the typical blocks in the wall.

Equation 1 gives the common form of relationship between size and strength.

$$Q_B = Q_o(V_B/V_o)^{-a} \qquad \text{eq 1}$$

where Q_B is the uniaxial compressive strength of a rock block of volume V_B, Q_o is the uniaxial compressive strength of a tested sample of volume V_o and 'a' is an exponent which depends on the particular rock. If detailed testing is not performed for 'a', 0.05 can be used and the standard deviation of Q_B can be assumed to be the same as that of Q_o.

Many pits are better approximated by assuming they are circular in shape rather than having constant cross section in a longitudinal direction. In Fig. 10, the results from a circular finite element model, i.e., with axisymmetric geometry, are shown. In these models, it was assumed that the horizontal field stresses are the same in all directions. The variation of the toe stresses with slope angle and with K, the ratio of horizontal to vertical field stresses, is shown. The toe stresses also vary with density of the wallrock, the height of the slope, and the radius of the pit measured at the crest.

Owing to the curvature of the walls, horizontal arching can occur. Such action will tend to decrease the toe stresses. As shown in Fig. 10, the effect for K = 1/3 is very slight owing to the dominant flow of stress being downward, the horizontal arching effect not operating in this direction. When K is equal to 1 and 3, the flow of the dominant stress will be in the horizontal direction, hence the arching effect will be significant, reducing the toe stresses below those that would be obtained for a straight wall, i.e., those under plane strain conditions. When the radius of curvature becomes very large, the axisymmetric case becomes very similar to the plane strain or long wall case.

The assumption of equal horizontal stresses in all directions is a special case. It would normally be assumed that the horizontal stresses would be a maximum in one direction and a minimum at 90° to that direction. Axisymmetric models were examined for two extreme stress conditions: first, assuming that the horizontal stress normal to the section of the wall being examined is zero and, second, assuming that the horizontal stress parallel to the section is zero.

Figure 11 shows the variation of toe stresses when the horizontal field stress normal to the section is zero. In this case, K, refers to the horizontal stress parallel to the section. It can be seen by comparing Fig. 10 and 11 that the horizontal field stress normal to the section has some influence on the maximum toe stresses.

In Fig. 12 the variation of the toe stresses is shown for cases where the horizontal

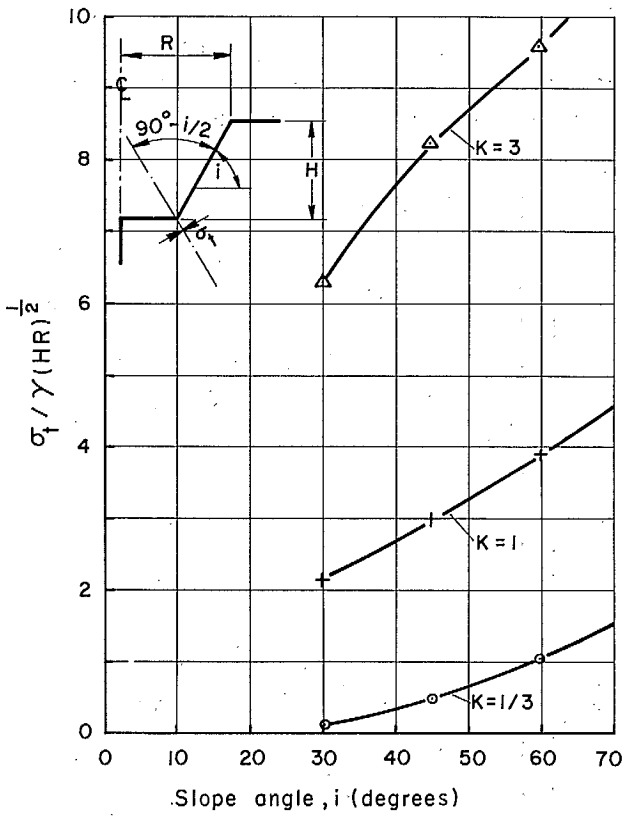

Fig. 10 - Variation of toe stresses, σ_t, with slope angle and K in an axisymmetric pit; the horizontal field stresses are the same in all directions; σ_t is at a point approximately 2 m in from the rock surface; K is the ratio of horizontal to vertical field stress; γ is the density of the rock mass; H is the height of the slope; R is the radius of the pit at the crest

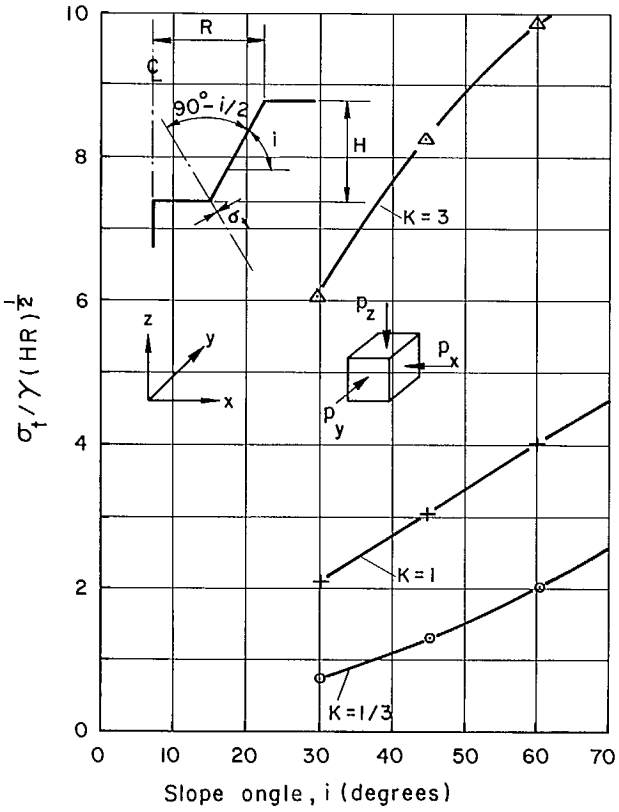

Fig. 11 - Variation of toe stresses, σ_t, with slope angle and K in an axisymmetric pit where the horizontal field stress normal to the section, p_y, is zero; σ_t is at a point approximately 2 m in from the rock surface; K is the ratio of maximum horizontal to vertical field stress; γ is the density of the rock mass; H is the height of the slope; R is the radius of the pit at the crest

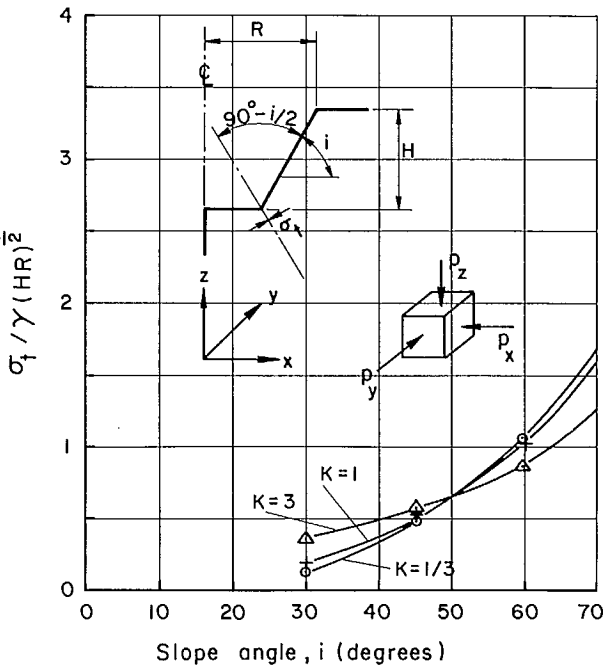

Fig. 12 - Variation of the toe stresses, σ_t, with slope angle and K in an axisymmetric pit where the horizontal field stress parallel to the section, p_x, is zero; σ_t is at a point approximately 2 m in from the rock surface; K is the ratio of maximum horizontal to vertical field stress; γ is the density of the rock mass; H is the height of the slope; R is the radius of the pit at the crest

stress parallel to the section is zero. In this case, K relates to the horizontal stress normal to the section being examined. It can be seen that the effect of K in these models is small, the stresses being caused principally by the vertical field stress. By using Fig. 10, 11 and 12, it is possible to estimate the toe stress for different combinations of horizontal field stresses acting in the directions perpendicular and parallel to the section being examined. For example, the horizontal stress in the rock of the footwall parallel to a cross section might be two times the vertical stress and in the direction perpendicular to the cross section it might be half the vertical stress. Then for an end wall, the reverse would exist giving rise to different toe stresses. The procedure will be shown below in an example.

It is conceivable that monitoring studies over a considerable period of time could show wall movement to be a sensitive indicator of impending unstable conditions. A critical deformation that immediately preceded instability might be identified. It is envisaged that the loosening and weakening effects of excavation and of blasting could be related to the movement of the crest towards the pit. No research has yet been

done to substantiate such a concept; however, Fig. 13, 14 and 15 give results from models so that field measurements can be compared with elastic movement. These figures are provided for those who decide to conduct such a field study. Furthermore, these curves must be used with some thought, e.g., where the models indicate negative horizontal movement, i.e., away from the pit, such movement could only be expected in a continuous, elastic medium. For typical jointed rock masses, such movement is unlikely to occur.

When block flow is considered to be the only potential mode of sliding, it will be necessary to produce schedules of variation of reliability with slope height for any selected slope angle. At the present time and for the foreseeable future, the most difficult problem in such an analysis is to determine the magnitude of the horizontal field stresses to be used for the determination of the critical stresses, e.g., toe stresses for a homogeneous formation. In many cases, the best that can be done is to make an estimate of K after a geological appraisal of the site. Under these circumstances, a relatively simple probability analysis is appropriate; although the results will be crude, the procedure makes best use of all the available information and provides a basis for establishing the ultimate pit design. The procedure can also highlight areas where further expenditure of funds is warranted to obtain critical information.

Because the nature of the available information on the horizontal field stresses, i.e., the direction of the principal stresses, their mean

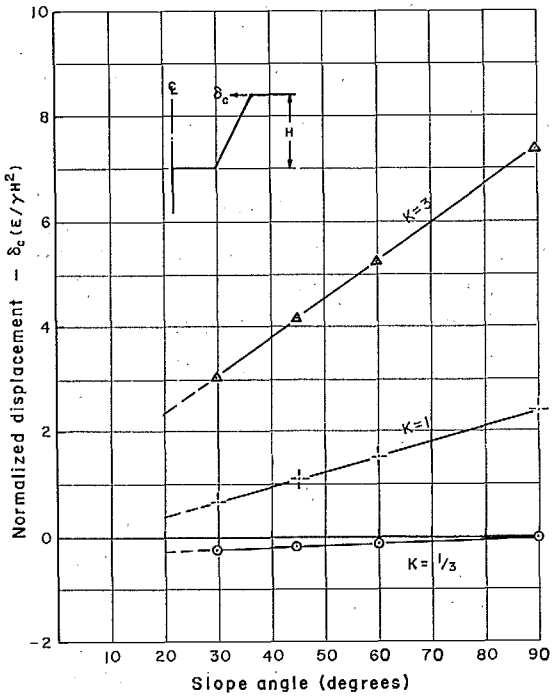

Fig. 13 - Variation of excavation displacements in plane strain; the horizontal displacement at the crest varies with slope angle and K, the ratio of horizontal to vertical field stress, as well as with slope height, H, rock mass density, γ, and modulus of deformation, E

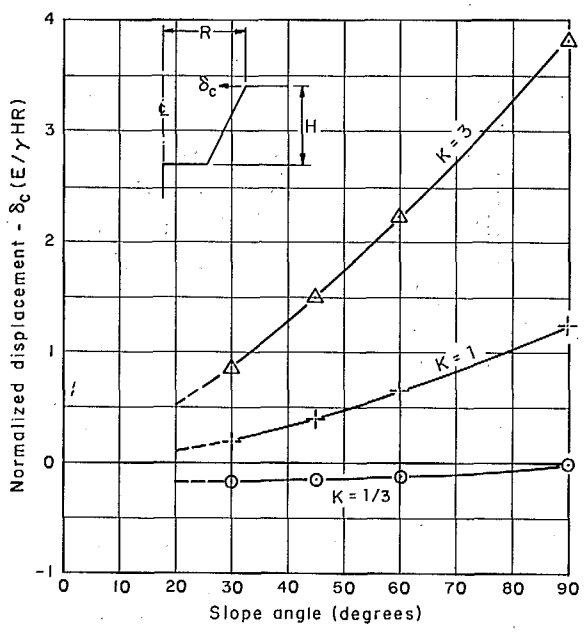

Fig. 14 - Variation of excavation displacements for an axisymmetric pit and axisymmetric field stresses; the horizontal displacement at the crest varies with slope angle and K, the ratio of horizontal to vertical field stress, as well as with slope height, H, rock mass density, γ, modulus of deformation, E, and radius of the pit at the crest, R

values, and their standard deviations are only approximate and vary widely as shown in studies at mines across Canada, it is only reasonable to ignore variations of other parameters, excluding strength. The effect of these is insignificant compared with that of the variance in K.

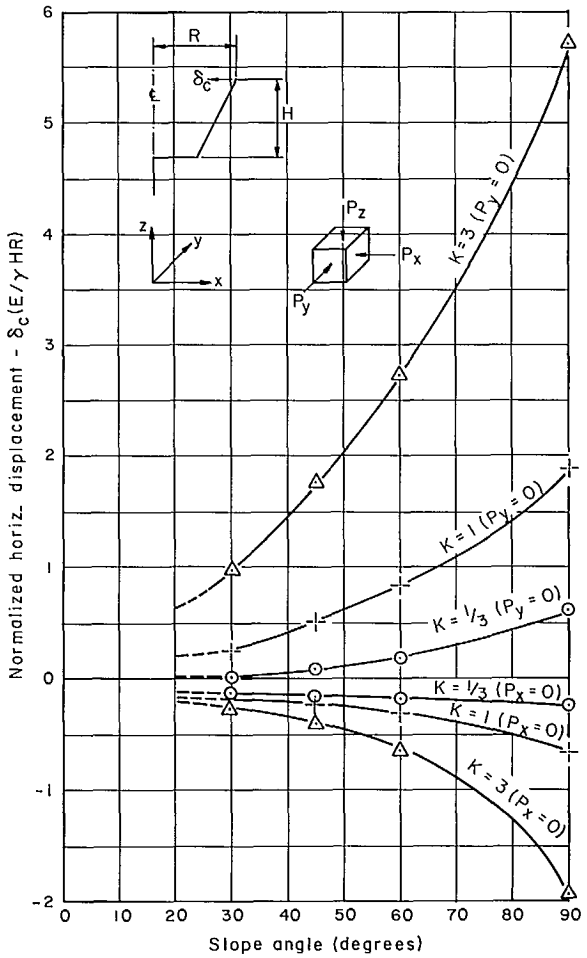

Fig. 15 - Variation of excavation displacements for an axisymmetric pit but non-axisymmetric field stresses; the horizontal displacement at the crest varies with slope angle and K, the ratio of horizontal to vertical field stress as well as p_x, the horizontal field stress parallel to the section, p_y the horizontal field stress normal to the section, slope height, H, rock density, γ, modulus of deformation, E, and radius of the pit at the crest, R

The procedure for determining the mean critical height, its standard deviation, and reliability of the pit wall at various heights is as follows:

a. Select a slope angle, i, assuming the following parameters are known: (1) the geometry of the pit, i.e., whether it can be approximated by a long wall or by a circular plan; (2) the ratio of horizontal to vertical field stresses, K, (both mean and standard deviations); (3) the density of the rock mass, γ; (4) the radius of the pit at the crest if it is circular, R; and (5) the mean, M_Q, and standard deviations, S_Q, of the uniaxial compressive strength of the rock substance, Q.

b. Determine from Fig. 9 and 10 or a combination of Fig. 10, 11 and 12, using i from above, the mean values of K, M_K, and y, M_y. Note that y is a dimensionless variable that includes toe stress and slope height. The standard deviation, S_y, is obtained by subtracting S_K from M_K, reading off the corresponding y-ordinate and then substracting it from M_y to give S_y.

c. Calculate the mean critical height, assuming this occurs when the mean stress, σ_t, is equal to the mean uniaxial compressive strength of the rock substance, M_Q. Hence $\sigma_t = Q$. For a long slope, or a plane strain condition, from Fig. 8, $y = \sigma_t/\gamma H = Q/\gamma H$, or $H = Q/\gamma y$. The mean critical slope height is obtained from the equation:

$$M_H = M_Q/\gamma M_y \qquad \text{Eq 2}$$

The standard deviation for the height is obtained from the statistics equation (2):

$$S_H = M_H[(S_Q/M_Q)^2 + (S_y/M_y)^2]^{\frac{1}{2}} \qquad \text{Eq 3}$$

For axisymmetric slopes at the critical height, $y = \sigma_t/(HR)^{\frac{1}{2}} = Q/\gamma(HR)^{\frac{1}{2}}$, or $H = (Q/\gamma y)^2/R$. The critical slope height is then obtained from statistics equations, i.e., if $a = X^2/M_a = M_X^2 + S_X^2$ and $S_a = 2M_X S_X$ (2); let $X = Q/\gamma y$ and using Eq 2 and 3, we have:

$$M_X = M_Q/(\gamma M_y)$$

and $S_x = M_x[(S_Q/M_Q)^2 + (S_y/M_y)^2]^{\frac{1}{2}}$

Therefore $M_H = (M_x^2 + S_x^2)/R$ Eq 4

$S_H = 2 M_x S_x /R$ Eq 5

d. For a series of interim slope heights, calculate the z-factor from the following equation: $z = (M_H - H)/S_H$, and then determine the reliability or the probability of instability, P_f, from Table 1.

e. Select a second feasible slope angle and repeat the steps from a to d; likewise for third and fourth trials if appropriate.

EXAMPLES

The first example is for a pit where one design sector is part of a long wall. It is thus considered to be in a state of plane strain. The mean uniaxial compressive strength of the rock substance, M_Q, is 20,000 psi (138 MPa), and the standard deviation, S_Q, is 8000 psi (55 MPa). The density of the rock mass, γ, is 165 pcf (2640 kg/m^3). The mean value, M_K, is 3, and the standard deviation, S_K, is 1. The maximum slope height is to be 1000 ft (305 m). To provide schedules of reliability or probability of instability versus slope height for a series of slope angles, the above procedure is followed.

a. Try i = 55°.

b. From Fig. 9, M_y = 15.9 and S_y = 4.9 (i.e., the interpolated difference for y between K = 3 and K = 2).

c. From Eq 2:
M_H = 20,000 x 144/(165 x 15.9)
= 1098 ft (335 m)

From Eq 3:
$S_H = 1098\ [(8000/20,000)^2 + (4.9/15.4)^2]^{\frac{1}{2}}$
= 554 ft (169 m)

d. For each intermediate height, the z-factor and probability of instability is determined, using Table 1, as follows:

H = 200 ft (61m), z = (1098 -200)/554 = 1.62
P_f = 5.3%

H = 400 ft (122m), z = (1098 -400)/554 = 1.26
P_f = 10.4%

H = 600 ft (183m), z = (1098 -600)/554 = 0.90
P_f = 18.4%

H = 800 ft (244m), z = (1098 -800)/554 = 0.54
P_f = 29.5%

H = 1000 ft (305m), z = (1098 -1000)/554 = 0.18
P_f = 42.9%

e. Try i = 50°.
M_y = 14.8, S_y = 4.7
M_H = 20,000 x 144/(165 x 14.8)
= 1179 ft (360m)
$S_H = 1179\ ((8000/20,000)^2 + (4.7/14.8)^2)^{\frac{1}{2}}$
= 602 ft (184 m)

H = 200 ft (61m), z = (1179 -200)/602 = 1.63
P_f = 5.2%

H = 400 ft (122m), z = (1179 -400)/602 = 1.29
P_f = 9.9%

H = 600 ft (183m), z = (1179 -600)/602 = 0.96
P_f = 16.9%

H = 800 ft (244m), z = (1179 -800)/602 = 0.63
P_f = 26.5%

H = 1000 ft (305m), z = (1179 -1000)/602 = 0.30
P_f = 38.2%

The probability of instability for several slope angles, i = 35°, 45°, 50°, 55°, and 60° is plotted and shown in Fig. 16.

The second example is for a circular pit, with axisymmetric geometry. The design sector under consideration is on the north wall. The mean uniaxial compressive strength of the rock substance is 20,000 psi (138 MPa) and the standard

Table 1: Standardized normal distributions

$z = (M-x)/S$ $z = (x-M)/S$	$R = 1-P_f$ P_f	P_f $R = 1-P_f$
0.0	0.5000	0.5000
0.1	0.5398	0.4601
0.2	0.5793	0.4207
0.3	0.6179	0.3820
0.4	0.6554	0.3445
0.5	0.6915	0.3085
0.6	0.7257	0.2742
0.7	0.7580	0.2419
0.8	0.7881	0.2118
0.9	0.8159	0.1840
1.0	0.8413	0.1586
1.1	0.8643	0.1356
1.2	0.8849	0.1150
1.3	0.9032	0.0968
1.4	0.9192	0.0807
1.5	0.9332	0.0668
1.6	0.9452	0.0547
1.7	0.9554	0.0445
1.8	0.9641	0.0359
1.9	0.9713	0.0287
2.0	0.9772	0.0227
2.1	0.9821	0.0178
2.2	0.9861	0.0139
2.3	0.9893	0.0107
2.4	0.9918	0.0081
2.5	0.9938	0.0062
2.6	0.9953	0.0046
2.7	0.9965	0.0034
2.8	0.9974	0.0025
2.9	0.9981	0.0018

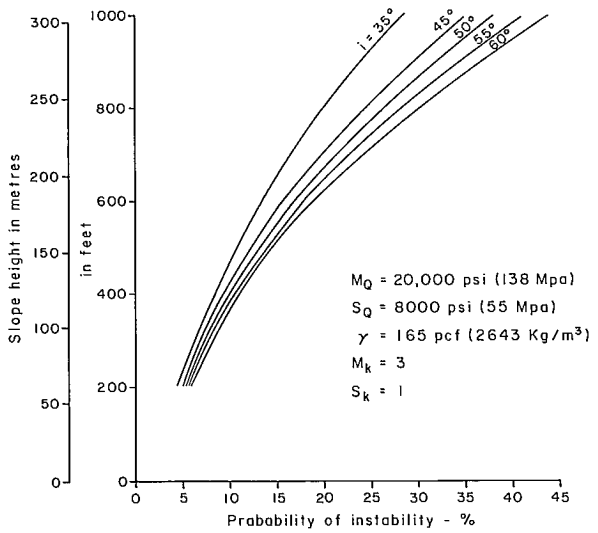

Fig. 16 - Probability of instability versus slope height for a longwall or plane strain slope

deviation 8000 psi (55 MPa). The density of the rock mass in the wall is 165 pcf (2640 kg/m³). The maximum height of the wall is to be 1000 ft. The radius of curvature of the wall at the crest, R, is 900 ft (270 m). The mean ratio of the horizontal field stress, p_x, to the vertical stress in the north/south plane is 3 and its standard deviation is 1; the horizontal stress, p_y, in the east/west direction is one half that in the north/south direction.

Note that the toe stress, or y-ordinate in the graphs $\sigma_t/\gamma(HR)^{\frac{1}{2}}$, can be considered to be composed of the following three elements: $y = A+B+C$, where A varies with the vertical stress, B varies with the horizontal stress in the north/south direction, and C varies with the horizontal stress in the east/west direction.

To provide schedules of reliability versus slope height for a series of slope angles, the same general procedure is followed.

a. Let i = 55° for a first trial.

b. From Fig. 10 for K = 3 and i = 55°,
$y = 9.2 = A + B + C$.

c. From Fig. 11 for K = 3 and i = 55°,

$y = 9.6 = A+B$ and therefore $C = -0.4$.

From Fig. 12 for $K = 3$, $y = 0.78 = A+C$, and therefore $A = 1.18$ and $B = 8.4$.

But $y' = A+B+C'$ where C' is for $p_y/p_x = 0.5$; in other words, the effect of p_y is only half of that acting on the models of Fig. 10.

From Fig. 12 for $K = 3/2 = 1.5$, $y' = 0.82$, and therefore $C' = y' - A = 0.82 - 1.18 = -0.36$.

Therefore, for the given stress conditions $M_y = 1.18 + 8.4 - 0.36 = 9.2$. For S_y determine y' for $M_K - S_K = 3 - 1 = 2$.
From Fig. 10 for $K = 2$, $y = 6.4 = A+B+C$.
From Fig. 11 for $K = 2$, $y = 6.7 = A+B$, and therefore $C = -0.3$
From Fig. 12 for $K = 2$, $y = 0.81 = A+C$, and therefore $A = 1.11$ and $B = 5.6$.
From Fig. 12 for $K = 2/2 = 1$, $y' = 0.88$ and $C' = -0.23$
$S_y = 9.2 - 6.5 = 2.7$.

d. From Eq 4 and 5 we have:
$M_H = (M_x^2 + S_x^2)/R$ and

$S_H = 2M_xS_x/R$, where

$M_x = M_Q/(\gamma M_y)$ and

$S_x = M_x[(S_Q/M_Q)^2 + (S_y/M_y)^2]$. Therefore

$M_x = 20{,}000 \times 144/(165 \times 9.2)$

$= 1897$ ft (579 m) and

$S_x = 1897\ [(8000/20{,}000)^2 + (2.79.2)^2]^{\frac{1}{2}}$

$= 941$ ft (287 m).

$M_H = (1897^2 + 941^2)/900 = 4982$ ft (1520 m).

$S_H = 2 \times 1897 \times 941/900 = 3967$ (1210 m).

e. To determine probability of instability for each intermediate height, the z-factor is calculated and Table 1 used.

H = 200 ft (61m), z = (4982 -200)/3967 = 1.21
P_f = 11.3%

H = 400 ft (122m), z = (4982 -400)/3967 = 1.16
P_f = 12.3%

H = 600 ft (188m), z = (4982 -600)/3967 = 1.10
P_f = 13.6%

H = 800 ft (244m), z = (4982 -800)/3967 = 1.05
P_f = 14.7%

H = 1000 ft (305m), z = (4982 -1000)/3967 = 1.00
P_f = 15.9%

Although these probability schedules are not likely to be very precise, they provide a means of appraising the effects of incremental slope changes on benefits and costs. They could be used as input into financial programs (3). However, the entire paper is more in the nature of a starting point for analyzing this type of instability. More research and analyses will be done before an established engineering tool is available.

REFERENCES

1. Yu, Y.S. and Coates, D.F. "Analysis of rock slopes using the finite element method"; CANMET Research Report R229; 1970.

2. Coates, D.F. "Pit Slope Manual, Chapter 5 - Design"; CANMET Report 77-5, 126 p, (Appendix A); March 1977.

3. Kim, Y.C. et al "Pit Slope Manual Supplement 5-3 - Financial Computer Programs"; CANMET Report 77-6, 184 p; May 1977.

CANMET REPORTS

Recent CANMET reports presently available or soon to be released through Printing and Publishing Supply and Services, Canada (addresses on inside front cover), or from CANMET Publications Office, 555 Booth Street, Ottawa, Ontario K1A 0G1:

Les récents rapports de CANMET, qui sont présentement disponibles ou qui ce seront bientôt peuvent être obtenus de la direction de l'Imprimerie et de l'Edition, Approvisionnements et Services, Canada (adresses au verso de la page couverture), ou du Bureau de Vente et distribution de CANMET, 555 rue Booth, Ottawa, Ontario, K1A 0G1:

77-14 Pit slope manual - Chapter 7 - Perimeter blasting; P. Calder;
Cat. No. M38-14/7-1977, ISBN 0-660-01011-9; Price: $2.25 Canada, $2.70 other countries.

77-16 Pit slope manual - Supplement 5-1 - Plane shear analysis; O.F. Coates;
Cat. No. M38-14/5-1977-1, ISBN 0-660-01008-9; Price: $4.25 Canada, $5.10 other countries.

77-19 Pit slope manual - Supplement 2-2 - Domain analysis programs; O. Cruden and J. Ramsden;
Cat. No. M38-14/2-1977-2, ISBN 0-660-00990-0; Price: $3.75 Canada, $4.50 other countries.

77-23 Pit slope manual - Supplement 2-4 - Joint mapping by terrestrial photogrammetry; G. Herget;
Cat. No. M38-14/2-1977-4, ISBN 0-660-00992-7; Price: $2.50 Canada, $3.00 other countries.

77-24 Pit slope manual - Supplement 2-5 - Structural geology case history; G. Herget;
Cat. No. M38-14/2-1977-5, ISBN 0-660-00993-5; Price: $2.75 Canada, $3.30 other countries.

77-30 Pit slope manual - Supplement 4-1 - Computer manual for seepage analysis; J. Marlon-Lambert;
Cat. No. M38-14/4-1977-1, ISBN 0-660-01007-0; Price: $3.50 Canada, $4.20 other countries.

77-31 Pit slope manual - Supplement 10-1 - Reclamation by vegetation - Vol. 1 - Mine waste description and case histories; O. Murray;
Cat. No. M38-14/10-1977-1, ISBN 0-660-01013-5; Price: $3.50 Canada, $4.20 other countries.

77-47 Statistical correlation of ASTM and JIS coke tumbler test results; W.R. Leeder and K.A. Jonasson;
Cat. No. M38-13/77-47, ISBN 0-660-01705-9; Price: $1.25 Canada, $1.50 other countries.

77-56 Corrosion protection and lateral displacement characteristics of rock anchors; R. Sage;
Cat. No. M38-13/77-56, ISBN 0-660-01806-3; Price: $1.25 Canada, $1.50 other countries.

77-58 Pit slope manual - Supplement 10-1 - Reclamation by vegetation - Vol. 2 - Mine waste inventory by satellite imagery; O. Murray;
Cat. No. M38-14/10-1977-1-2, ISBN 0-660-01464-5; Price: $6.00 Canada, $7.20 other countries.

77-60 The high-temperature behaviour of blast furnace coke - A review; O.A. Reeve, J.T. Price and J.F. Gransden;
Cat. No. M38-13/77-60, ISBN 0-660-01807-1; Price: $1.25 Canada, $1.50 other countries.

77-61 A rapid method for the determination of sulphur and vanadium in petroleum products by non-dispersive x-ray fluorescence; R. Makhija, R.G. Draper and E. Furmisky;
Cat. No. M38-13/77-61, ISBN 0-660-01848-9; Price: $1.00 Canada, $1.20 other countries.

77-65 Performance of superplasticizers in concrete: Laboratory investigation - Part 1; V.M. Malhotra and O. Malanka;
Cat. No. M38-13/77-65, ISBN 0-660-01739-3; Price: $1.75 Canada, $2.10 other countries.

78-2 Revision of recommended values for reference ores MP-1 and KC-1; G.H. Faye and W.S. Bowman;
Cat. No. M38-13/78-2, ISBN 0-660-01712-1; Price: $1.00 Canada, $1.2 other countries.

78-3 Certified and provisional reference materials available from the Canada Centre for Mineral and Energy Technology, 1978; G. Faye;
Cat. No. M38-13/78-3, ISBN 0-660-01804-7; Price: $1.25 Canada, $1.50 other countries.

76-40F Evaluation des charbons marchands canadiens: Nouvelle-Ecosse et Nouveau Brunswick - 1975; T.E. Tibbetts et W.J. Montgomery;
Cat. No. M38-13/76-40F, ISBN 0-660-01821-7; Price: $3.00 Canada, $3.60 other countries.